RESEARCH PAPERS

The Interface-Modulated Structure of $TaSi_{0.360}Te_2$

By A. van der Lee, M. Evain, L. Monconduit, R. Brec and J. Rouxel

IMN, Laboratoire de Chimie des Solides, 2 Rue de la Houssinière, 44072 Nantes CÉDEX 03, France

and V. Petříček

Institute of Physics, Academy of Sciences of the Czech Republic, Na Slovance 2, 180 40 Praha 8, Czech Republic

Abstract

The incommensurate modulation in the structure of $TaSi_{0.360}Te_2$ has been determined by single-crystal X-ray diffraction. The $(3 + 1)$-dimensional superspace group is $Pnma(00\gamma)s00$, $\gamma = 0.3602$ (8), basic unit-cell dimensions $a = 6.329$ (3), $b = 14.031$ (3), $c = 3.8258$ (7) Å, $V = 339.72$ Å^3, $Z = 4$. Refinement on 1907 reflections with $I \geq 2.5\sigma(I)$ converged to $R = 0.097$, $R = 0.064$ for 521 main reflections, $R = 0.089$ for 831 first-order satellites and $R = 0.174$ for 555 second-order satellites. The structure can be regarded as based upon the structure of the commensurate parent compound $TaSi_{1/3}Te_2$ modulated by the incommensurate insertion of interfaces consisting of units of the hypothetical orthorhombic commensurate compound $TaSi_{1/2}Te_2$. All individual occupation probability and displacement waves show a strong block-wave character. For the occupation probability waves, the parameters of a step function are used in the refinements and compared with those resulting from a conventional refinement based upon Fourier components. A number of Te—Te contacts can be identified as bonding. This is explained by a charge transfer from the Te p-block bands to the Ta d-block bands.

Introduction

The tendency of Te atoms to form short bonds in transition-metal tellurides has received much attention during the past few years (Böttcher, 1988; Jobic, Brec & Rouxel, 1992; Mar, Jobic & Ibers, 1992; Canadell, Jobic, Brec, Rouxel & Whangbo, 1992; Canadell, Monconduit, Evain, Brec, Rouxel & Whangbo, 1993; Rouxel, 1993). For instance, Te—Te contacts shorter than the van der Waals distance of about 4.0 Å are rather common in many transition-metal tellurides. Electronic structure stud-ies of these compounds have shown that, due to the significant electron transfer from the Te p orbitals to the transition-metal element d bands, the formal oxidation state of Te is in general smaller than -2 (Canadell *et al.*, 1992; Canadell *et al.*, 1993), *e.g.* -1.5 for the $Ir_n^{3+}(Te^{-1.5})_{2n}$ family of structures (Jobic *et al.*, 1992). The ability of Te to adopt oxidation states intermediate between -1 and -2 leads to a great variability of the anionic bonding compared with the less covalent sulfur and selenium compounds.

The syntheses and characterization of compounds in the M—A—Te system (M = Ta, Nb and A = Si, Ge) have opened the possibility to change the fractional oxidation number of Te on an almost continuous scale by changing the relative stoichiometry of the compound and thus to monitor electronic *versus* structural changes rather accurately. Hitherto, the phases Nb_2SiTe_4 (Monconduit, Evain, Brec, Rouxel & Canadell, 1993), Nb_3SiTe_6 (Li, Badding & DiSalvo, 1992), Nb_3GeTe_6 (Li & Carroll, 1992; Monconduit, Evain, Boucher, Brec & Rouxel, 1992), Ta_3SiTe_6 (Evain, Monconduit, Van der Lee, Brec, Rouxel & Canadell, 1993), $Nb_7Ge_3Te_{14}$ (Van der Lee, Evain, Monconduit, Brec & van Smaalen, 1994) and $Nb_5Ge_2Te_{10}$ (Van der Lee, Mansuetto, Evain, Monconduit, Brec & Rouxel, 1994) have been synthesized and studied by X-ray diffraction and electronic band-structure calculations. The phases are unique in the sense that A is fourfold coordinated in the middle of the common face of two trigonal Te prisms. M is found in the middle of trigonal Te prisms; a specified fraction of the transition-metal atoms forms bonded pairs through the common face of two trigonal prisms. The overall structure can be seen as a close stacking of Te—Te sandwiches in an orthorhombic AA/BB mode for M_3ATe_6 and $M_7A_3Te_{14}$, a monoclinic AA/BB mode for $M_5A_2Te_{10}$ and in a monoclinic $AA/BB/CC$ mode for Nb_2SiTe_4.

The van der Waals gap between successive Te sand-wiches is empty. All structures, whether the stacking is AA/BB or $AA/BB/CC$, can be regarded as based upon a small basic unit cell in which the cation sites are under occupied (Fig. 1). For the orthorhombic mode, the positions of the atoms are described in the space group $Pnma$ (No. 62, *International Tables for Crystallography* (1983, Vol. A) with $M(1)$ at $4(c)$ ($\sim 0,\frac{1}{4},\sim 0.3$), $M(2)$ at $4(c)$ ($\sim 0,\frac{1}{4},\sim 0.0$), A at $4(c)$ ($\sim 0.43,\frac{1}{4},\sim 0.31$), and Te at $8(d)$ ($\sim 0.17,\sim 0.12,\sim 0.48$). The sum of the occupancies of the $M(1)$ site and the $M(2)$ site amounts to 1.00, whereas the occupancy of the A site is almost equal to that of the $M(2)$ site. Variations in the ratio between the occupancies of the $M(1)$ site and the $M(2)$ site may give rise to different modulated super-structures, *e.g.* the phases M_3ATe_6, $M_5A_2Te_{10}$ and $M_7A_3Te_{14}$ are commensurately modulated super-structures of the basic unit cell of Fig. 1 with wave-vectors $q = \frac{1}{3}c$, $q = \frac{2}{5}c$, and $q = \frac{3}{7}c^*$, respectively. The modulation results from the ordering of the cations accompanied by a strong distortion of the Te sheets. A monoclinic mode can arise because of a shift of the 'filling' of a Te sandwich or a shift of the complete Te sandwich with respect to the other sandwiches. To clarify the similarity between the structures of the M—A—Te compounds, the structure formula will be written as MA_xTe_2, or more elaborated as $M(1)_{1-x}M(2)_xA_xTe_2$, where x might take rational (written as n_1/n_2) or irrational values.

In this work we present a model for the incommensurately modulated structure of $TaSi_{0.360}Te_2$. It is shown that the structure is similar to that of $Nb(Ta)Si_{1/3}(Ge)Te_2$, except for the quasi-periodic insertion of (001) faults of the hypothetic ortho-rhombic $MA_{1/2}Te_2$ structure type. The occupation

Fig. 1. Projection of one sandwich of the basic unit cell of modulated structures of MA_xTe_2 (M = Ta, Nb; A = Ge, Si) compounds. Te atoms form a hexagonal network, M atoms are in pairs and A atoms are lone. The radius of the circles representing the atoms is proportional to their occupation probability.

waves of the cations are analyzed with a conven-tional superposition of harmonics as well as with an ideal block wave.

Experimental

The phase under study was obtained in an attempt to prepare $TaSi_{1/2}Te_2$. Stoichiometric amounts of the elements were placed in an evacuated silica tube. The temperature was raised at $100\,K\,h^{-1}$, then main-tained for 10 d at 1225 K and finally lowered by exposure of the tube to room-temperature air. The analysis, by Weissenberg photographs, of the very thin dark platelets that were found in the batch showed that $TaTe_2$ had formed besides crystals with a basic unit cell close to that of $TaSi_{1.3}Te_2$, but with the spots due to the modulation slightly displaced from their ideal commensurate positions at $\frac{1}{3}c^*$ and $\frac{2}{3}c^*$ from the main reflections. Besides rather strong first-order satellites, weaker second-order satellites could also be identified. Note that for the commen-surate diffraction pattern with $q = \frac{1}{3}c^*$ second-order satellites of the reflection (h,k,l) coincide with the negative first-order satellite of $(h,k,l + 1)$. Thus, in total, two satellites are found in between two succes-sive main reflections along c^*, whereas for the incommensurate diffraction pattern with wavevector $q = (\frac{1}{3} + \delta)c^*$, in total four first- and second-order satellites are found.

Data collection was performed on an Enraf–Nonius CAD-4F diffractometer (see Table 1 for the recording conditions). The wavevector was determined from a least-squares refinement (Evain, 1992) of the positions obtained from the accurate centering of 38 strong first-order satellites: $q = 0.3602\,(8)c^*$. The measured intensities were corrected for the scale variation and Lorentz–polarization effects. A Gaussian absorption program was applied using the program *ABSORB* from the *XTAL* system (Hall, Flack & Stewart, 1992). Because of the large relative error of the measurement of the thickness of the very thin platelet, the final refinements were repeated with data sets corrected for absorption with different thicknesses until a minimal R factor was reached. The final thickness is 0.0036 mm. Symmetry-related reflections were averaged accord-ing to Laue symmetry mmm, yielding an internal consistency factor based upon observed reflections of $R_I = 0.033$. A final number of 1907 reflections with intensities $I > 2.5\sigma(I)$ was used for the refinements. Five reflections have been skipped from the refinements due to very large $\Delta(F_{calc} - F_{obs})$. This could be related to a low glancing angle with respect to the main face of the crystal and thus to an inadequate absorption correction. The omission of these reflections did not have any influence on the final parameters.

Table 1. *Crystal data of* $TaSi_{0.360}Te_2$ *and conditions of measurement*

Formula weight	446.5
Calculated density (g cm^{-3})	8.729
$F(000)$	728
Linear absorption coefficient (cm^{-1})	513.5
Maximum correction	11.66
Minimum correction	1.19
Crystal size (mm^3)	$< 0.12 \times 0.0036 \times 0.12$
Diffractometer	Enraf–Nonius CAD-4F
Temperature (K)	295
Radiation	Mo $K\alpha$
Scan mode	$\omega/2\theta$
Recording range ($^\circ$)	1.50–35.00
hklm range	$-1 < h < 11$, $-1 < k < 23$, $-7 < l < 7$ for $m = 0$ $-1 < l < 7$ for $m \neq 0$ $-3 < m < 3$
Standard reflections	002, 008, 200 every 3600 s

Symmetry and structure refinement

The systematic absences of the diffraction pattern pointed to the (3 + 1)-dimensional superspace group $Pnma(00\gamma)s00$. This superspace group can be shown to be equivalent to $Pnma(00\gamma)$ (No. 62.1 of Table 9.8.3.5 of *International Tables for Crystallography*, 1992, Vol. C) by the choice of the equivalent wavevector $\mathbf{q} = \mathbf{q} - \mathbf{c}^*$. We prefer, however, to use the shortest wave vector possible, since this makes the indexing of the diffraction pattern more transparent.

Refinements were started with only the main reflections and without any modulation parameters included, *i.e.* on the basic structure. Starting values for the atomic positions in the basic unit cell were calculated from the supercell coordinates of the structure of $TaSi_{1/3}Te_2$ (Evain *et al.*, 1994). The thermal parameters (the old phrase is used here instead of the more correct phrase 'atomic displacement parameter' so as not to confuse it with the amplitudes of the displacive waves) for all atoms were kept isotropic to avoid bias in the refinement of the modulated structure. In addition, the occupation probabilities of Ta(1), Ta(2) and Si were refined, but with the total occupation probability of Ta(1) and Ta(2) fixed to 1.00. The scattering factors for neutral atoms and the anomalous dispersion correction parameters were taken from *International Tables for X-ray Crystallography* (1974, Vol. IV). All refinements have been performed with the computing system *JANA*93 (Petříček, 1993). Plots of the structure have been made with the *ORTEP* program from the *XTAL* system (Hall *et al.*, 1992), whereas plots of the (derived) modulation functions have been made with a local version of *MISTEK* (van Smaalen, 1993). All refinements were based on $|F_{obs}|$ and performed in the full-matrix mode, using $w = 1/$ $[\sigma^2(|F_{obs}|) + 0.02(|F_{obs}|)^2]$ as weights. The refinement of the basic structure converged to $R = 0.191$ and $wR = 0.231$.

The modulated structure, as can be expected from the superstructures of Ta_3SiTe_6 and Nb_3GeTe_6, consists of a strong modulation of the occupation probability of Ta(1), Ta(2) and Si, and of the basic coordinates of Te. Displacive modulation waves for Ta(1), Ta(2) and Si have to be considered as well. Since the latter atoms are located on the m_y mirror plane [with (3 + 1)-dimensional symmetry operation $(x_1, \frac{1}{2} - x_2, x_3, x_4)$], the displacive modulation function perpendicular to this plane is strictly null.

The modulation functions can be taken as a limited number of harmonics from a Fourier series. The following definition has been used for the displacive modulation functions and the occupation probability modulation function, respectively,

$$\mathbf{r}^v(\bar{x}_4) = \mathbf{r}_0^v + \sum_{n=1}^{ntot} [\mathbf{u}_{s,n}^v \sin(2\pi n\bar{x}_4) + \mathbf{u}_{c,n}^v \cos(2\pi n\bar{x}_4)] \quad (1)$$

$$P^v(\bar{x}_4) = P_0^v + \sum_{n=1}^{ntot} [P_{s,n}^v \sin(2\pi n\bar{x}_4) + P_{c,n}^v \cos(2\pi n\bar{x}_4)] \quad (2)$$

where v counts the independent atoms in the basic unit cell. $\bar{x}_4$ is the argument of the modulation function $\bar{x}_4 = t + \mathbf{q}.\mathbf{r}_{0,L}^v = t + \mathbf{q}.(\mathbf{r}_0^v + \mathbf{L})$, with t the global phase of the modulation wave, $\mathbf{r}_0^v$ the average position within the basic unit cell, $\mathbf{L}$ denotes a basic structure lattice translation and $\mathbf{u}_{s,n}^v = (A_{x,s,n}^v, A_{y,s,n}^v, A_{z,s,n}^v)$, $\mathbf{u}_{c,n}^v = (A_{x,c,n}^v, A_{y,c,n}^v, A_{z,c,n}^v)$. In a first approach only the first two terms (ntot = 2) were considered since only first- and second-order satellites have been measured. The amplitudes of the occupation probability modulation function of Ta(1) and Ta(2) were restricted to each other by virtue of the conditions $P_{s,n}^{Ta(1)} = -P_{s,n}^{Ta(2)}$ and $P_{c,s}^{Ta(1)} = -P_{c,n}^{Ta(2)}$. Along with the restrictions on the average occupation probabilities $P_0^{Ta(1)} = 1.00 - P_0^{Ta(2)}$, this means that the sum of the occupation probabilities of Ta(1) and Ta(2) is kept constant for every value of the phase $\bar{x}_4$. This is a reasonable restriction since it implies that the sum of the occupation probabilities of the two Ta sites that are very close to each other throughout the modulated structure [since $\langle |\mathbf{r}_{0,L}^{Ta(1)} - \mathbf{r}_{0,L}^{Ta(2)} \rangle \approx \langle |\mathbf{r}_0^{Ta(1)} - \mathbf{r}_0^{Ta(2)}| \rangle \approx 1.1$ Å] is kept equal to 1.00

We first refined the first-order harmonics of the displacive modulation function of Te and the occupation probability modulation function of Ta(1) [the constrained function of Ta(2) 'follows'] against the intensities of the first-order satellites. In due course, we added the parameters of the other modulation functions and the intensities of the second-order satellites. The displacive wave of Si was confined to the first order in view of the small atomic number of Si compared with those of Ta and Te.

At this stage the refined set of Fourier amplitudes was carefully examined for its structural significance. This led us to pursue the refinement with three major adaptations, one concerning the waveform of the occupation probability modulation and the other two concerning the displacive waves. The first adaptation was tracked by plotting the occupation probability modulation function of Ta as a function of the phase. The waveform was found to be close to a block wave, or step function, i.e. for a definite interval of the phase $\bar{x}_4$ the value of the function is close to 1.0, whereas it is 0.0 outside this interval (Fig. 2). The maximum of the function amounted to 1.1 and the minimum to -0.2. Those chemically meaningless values do not necessarily imply that a penalty function should be used to constrain the occupation probability between 0.00 and 1.00 (Yamamoto, 1981). It only means that the intensities of the higher order satellites originating from the higher order harmonics are below the threshold of observability. Instead one may compare the results from a Fourier analysis of a suitable step function with the experimentally determined values of the amplitudes of the various harmonics and use the 'best' step function for the analysis of the modulated structure (Van der Lee, van Smaalen, Wiegers & de Boer, 1991), or one may try to refine the parameters of a step function.

The step function is mathematically defined as the difference between two Heaviside functions, one centered at the position of the step 'up', and the other at the position of the step 'down'. The Heaviside function itself is defined as

$$H(x) = 0 \text{ if } x < 0 \tag{3}$$

$$H(x) = 1 \text{ if } x > 0. \tag{4}$$

The step function for the occupation probability is accordingly

$$P(\bar{x}_4) = H(\bar{x}_4 - \bar{x}_{4,l}) - H(\bar{x}_4 - \bar{x}_{4,r}), \tag{5}$$

where $\bar{x}_{4,l} = \bar{x}_{4,0} - \Delta/2$ and $\bar{x}_{4,r} = \bar{x}_{4,0} + \Delta/2$. Δ, the width of the step, is just equal to the average occupation probability and $\bar{x}_{4,0}$ represents the center of the step. It is noted that the values of the Fourier amplitudes constituting the Fourier series of (2) can be calculated according to

$$P^v_{s,n} = \frac{1}{\pi n}[\cos{(2\pi \bar{x}^v_{4,l})} - \cos{(2\pi \bar{x}^v_{4,r})}] \tag{6}$$

$$P^v_{c,n} = \frac{1}{\pi n}[\sin{(2\pi \bar{x}^v_{4,r})} - \sin{(2\pi \bar{x}^v_{4,l})}]. \tag{7}$$

At this stage a clear distinction has to be made between displacive and occupation probability modulation functions regarding their influence on the magnitude of the structure factor. Van Aalst, Den Hollander, Peterse & de Wolff (1976) have

shown that in the case of a displacive modulation, the intensities of nth-order satellites are dominated by the Fourier amplitudes up to the nth order for relatively small displacements from the average structure. If the deviation from linearity becomes larger, Fourier amplitudes of the order greater than n might have a significant contribution to the intensities of order n. Using the same arguments as Van Aalst et al. (1976), one may show that in the case of an (pure) occupation probability modulation, the Fourier amplitudes of the nth order only contribute to the intensities of satellites of the nth order. This is because the occupation probability modulation function enters the expression of the structure factor as a prefactor of the exponential and not as a part of the argument, as for the displacive modulation function. Thus, the addition of higher order harmonics to the occupation probability modulation function without using the intensities of the corresponding satellites cannot be justified on the basis of the arguments given above. That we still want to use the concept of the step function of (3)–(5), which in principle involves the use of the intensities of an infinite number of higher order satellites, is because this function needs less refinable parameters than the standard function of (2) for the allowed number of harmonics.

The Fourier amplitudes of the displacive waves were also found to be relatively large and, therefore, we decided, employing the arguments of Van Aalst et al. (1976), to include the amplitudes of higher order harmonics in the expression of (1) as the second major adaptation to the initial refinement. Two different refinements were initiated, one using the
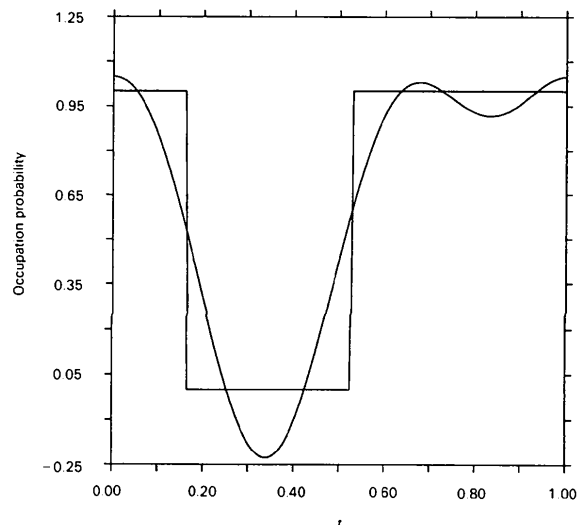
Fig. 2. Modulation function $P^{\text{Ta}(1)}(\bar{x}_4)$ versus $t = x_4 - \mathbf{q}.\mathbf{r}_0^v$, resulting from the refinement using two harmonics, and the final block wave utilizing the parameters of two Heaviside functions.

standard Fourier amplitudes up to the second order for the occupation probability modulation function, and the other using the parameters of the step function of (5), referred to as refinements I and II, respectively. Displacive Fourier amplitudes up to the fourth order for Te, up to the third order for Ta and up to the first order for Si were employed in both refinements. At the same time it appeared necessary to reduce the number of Fourier amplitudes for the displacive waves of Ta and Si because of the large correlations encountered between sine and cosine amplitudes. This is caused by the fact that the functions constituting the Fourier series of the displacive modulation function are not defined or ill-defined for the occupation probability functions of (2) and (5), respectively, for a certain interval of the phase, namely the section where the occupation probability is zero or close to zero. It is necessary to form an orthogonal set of functions out of the possible functions constituting the Fourier series of the displacive wave. The choice of using only cosine terms for the displacement waves of the cations as the third major adaptation to the initial refinement was found to be appropriate for the present case, although the chosen functions are not completely orthogonal to each other. The number of correlations has been diminished and the refinements are more stable. There remain, however, difficulties in the modelling of the displacement waves of the cations; the thermal parameter β_{33} of Ta is slightly negative. For Te, each adjunction of a higher order displacement wave did not affect much the parameters of the lower order displacement waves and significant amplitudes always resulted, thus showing the addition to be meaningful.

R factors of both refinements have been compiled in Table 2 and the refined parameters can be found in Tables 3 and 4 for both the conventional (I) and the step function refinement (II).*

Results and discussion

We start the discussion with a comparison between the results of the refinement based on harmonics only and that based upon the use of the step function for the occupation probability modulation waves. We will then focus on the overall distribution of the cations within the Te sandwiches. Finally we will pay attention to Te—Te bonding distances and discuss the results in terms of electronic transfer.

---

* Lists of observed and calculated structure factors for the conventional refinement and anisotropic thermal parameters have been deposited with the British Library Document Supply Centre as Supplementary Publication No. SUP 71579 (13 pp.). Copies may be obtained through The Technical Editor, International Union of Crystallography, 5 Abbey Square, Chester CH1 2HU, England.

Table 2. *Reliability factors for the two different models*

Reflection subset	No. of reflections	R*		wR*	
		I	II	I	II
$m = 0$	521	0.064	0.066	0.074	0.077
$m = 1$	831	0.089	0.091	0.096	0.099
$m = 2$	555	0.173	0.179	0.175	0.192
Overall	1907	0.097	0.099	0.105	0.110

*The *R* factors are defined as $R = \sum ||F_{obs}| - |F_{cal}||/\sum|F_{obs}|$ and $wR = [\sum w(|F_{obs}| - |F_{cal}|)^2/\sum w(|F_{obs}|)^2]^{1/2}$ with weights *w*. Partial *R* factors are defined with a subset of the reflections. Satellites of the order *m* are defined as $hklm_i$ reflections. I and II refer to the two different refinements mentioned in the text.

Step function versus truncated Fourier series

In Table 5, Fourier amplitudes resulting from refinement I are compared with those calculated from the width and the center of the step resulting from refinement II by employing (6) and (7). It is seen that the agreement between the first-order harmonics of Ta is excellent, the second-order harmonics showing more disagreement. From the table it is clear that the omission of fourth-order satellites most influences the fit, the amplitudes of the order > 5 being equal or smaller than those of the order 3. Very weak spots at positions expected for fourth-order satellites could be identified posteriorly on a long-exposure Weissenberg photograph, but at the time of data collection this was not recognised as such because of the reduction in intensity in going from first- to second-order satellites.

For Si the agreement between the values of the Fourier amplitudes is not so good, for P_0^{Si} as well as for $P_{s,n}^{Si}$ and $P_{c,n}^{Si}$. This is expected because of the small atomic weight of Si compared with Ta and Te, making its refinement behavior less stable. There are, however, several reasons to believe that the first- and second-order harmonics calculated from the parameters of the step function represent the actual situation more closely than those resulting from refinement I. The first reason is that strong correlations are expected to exist between P_0^{Si} and $P_{s,n}^{Si}$ and $P_{c,n}^{Si}$, in the same way as correlations exist between the thermal parameters and P_0^{Si}. At least the former correlations do not exist in refining the two parameters of the step function: Δ^{Si} is identical to P_0^{Si} and $\bar{x}_{4,0}^{Si}$ represents the offset of the step with respect to the arbitrarily chosen origin. The second reason is that the average occupation probability is expected to be close to that of Ta(2), as will be outlined in the next paragraph.

From Table 3 it follows that the Fourier amplitudes of the displacive modulation for Te hardly differ between the two refinements, but also that there are substantial differences between those for the occupationally modulated cations, even for the average coordinates r_0^{ν}. Some amplitudes are very

Table 3. *Final values for the amplitudes of the displacive modulation functions*

	n^*	$A^v_{x,c,n}$	$A^v_{y,c,n}$	$A^v_{z,c,n}$	$A^v_{x,s,n}$	$A^v_{y,s,n}$	$A^v_{z,s,n}$
Ta(1)							
	0				0.3213 (2)	0.25	-0.0382 (4)
					0.3208 (2)	0.25	-0.0390 (4)
	1	0.0	0.0	0.0	-0.0136 (3)	0.0	-0.0608 (5)
		0.0	0.0	0.0	-0.0130 (4)	0.0	-0.0600 (6)
	2	0.0	0.0	0.0	-0.0060 (4)	0.0	-0.0176 (8)
		0.0	0.0	0.0	-0.0075 (5)	0.0	-0.019 (1)
	3	0.0	0.0	0.0	-0.0018 (7)	0.0	0.005 (1)
		0.0	0.0	0.0	0.0013 (8)	0.0	0.008 (1)
Ta(2)							
	0				0.025 (2)	0.25	-0.020 (3)
					0.037 (4)	0.25	-0.001 (4)
	1	0.0	0.0	0.0	-0.008 (3)	0.0	0.093 (5)
		0.0	0.0	0.0	0.013 (8)	0.0	0.122 (8)
	2	0.0	0.0	0.0	-0.005 (3)	0.0	0.041 (4)
		0.0	0.0	0.0	0.012 (6)	0.0	0.064 (6)
	3	0.0	0.0	0.0	-0.003 (2)	0.0	0.033 (3)
		0.0	0.0	0.0	0.007 (3)	0.0	0.033 (4)
Si							
	0				0.435 (6)	0.25	0.34 (1)
					0.44 (1)	0.25	0.32 (2)
	1	0.0	0.0	0.0	0.016 (6)	0.0	0.09 (1)
		0.0	0.0	0.0	0.02 (1)	0.0	0.06 (3)
Te							
	0				0.1671 (2)	0.11676 (8)	0.4768 (3)
					0.1670 (2)	0.11676 (8)	0.4771 (3)
	1	0.0261 (3)	0.0013 (2)	0.0072 (5)	0.0187 (3)	-0.0022 (2)	-0.0189 (5)
		0.0261 (3)	0.0013 (2)	0.0073 (5)	0.0187 (3)	-0.0022 (2)	-0.0189 (5)
	2	0.0169 (3)	0.0006 (2)	0.0029 (7)	-0.0087 (3)	0.0020 (2)	0.0199 (6)
		0.0178 (3)	0.0006 (2)	0.0027 (7)	-0.0086 (3)	0.0021 (2)	0.0200 (6)
	3	0.0000 (6)	0.0004 (4)	0.005 (1)	0.0073 (6)	-0.0004 (4)	0.0002 (11)
		0.0005 (7)	0.0001 (4)	0.005 (1)	0.0076 (5)	-0.0002 (3)	-0.003 (1)
	4	-0.002 (1)	0.0004 (8)	-0.010 (2)	0.003 (1)	-0.0007 (7)	-0.008 (2)
		-0.0034 (9)	0.0005 (8)	-0.013 (2)	0.002 (1)	-0.0010 (7)	0.008 (2)

* The values on the first line of each n are from refinement I; those on the second line from refinement II. Experimental standard deviations are in parentheses.

Table 4. *Final values for the amplitudes of the occupation probability modulation waves*

	n	$P^v_{s,n}{}^*$	$P^v_{c,n}{}^*$	Δ^v	$\bar{x}^v_{4,0}$
Ta(1)	0		0.617 (2)	0.634 (2)	0.829 (1)
	1	-0.506 (4)	0.265 (4)		
	2	0.216 (4)	0.163 (4)		
Si	0		0.31 (3)	0.38 (2)	0.47 (1)
	1	-0.13 (4)	-0.73 (4)		
	2	-0.11 (4)	0.25 (5)		

* $P^v_{s,n}$ and $P^v_{c,n}$ result from refinement I, Δ^v and $\bar{x}^v_{4,0}$ from refinement II. Standard deviations are given in parentheses.

Table 5. *Comparison of principal harmonics from step function with refined harmonics*

	Ta(1)				Si			
	I		II		I		II	
n	$P^v_{s,n}$	$P^v_{c,n}$	$P^v_{s,n}$	$P^v_{c,n}$	$P^v_{s,n}$	$P^v_{c,n}$	$P^v_{s,n}$	$P^v_{c,n}$
0		0.617		0.634		0.329		0.375
1	-0.509	0.267	-0.511	0.278	0.126	-0.737	0.124	-0.575
2	0.217	0.164	0.199	0.129	-0.217	-0.164	-0.093	0.205
3			-0.005	0.065			-0.049	0.066
4			0.144	-0.065			0.112	-0.101
5			-0.051	-0.039			-0.042	0.023

large, *e.g.* $A^{Ta(2)}_{z,c,j}$, although the correlations have been diminished by setting all sine amplitudes to zero. It turns out that the three-dimensional coordinates in the modulated structure calculated with (1) are close to each other for both refinements if the occupancy probability is close to 1.00 or equal to 1.00, and that they are further apart if the occupancy probability is close to 0.00 or equal to 0.00. It must be kept in mind that the displacive modulation functions are defined for the complete period of the phase, but that they are meaningless for those intervals where the occupation probability is close to 0.00. Thus, the two

sets of functions may differ for those intervals and that difference gives rise to a different mean r^v_0.

Taking into account the observations made in this paragraph, we have a slight preference for the model based upon the refinement of the parameters of the step function, although the R factors are a little worse. The occupational modulation wave from refinement I is close to a block wave, as can be inferred from Fig. 2, but still all occupancies between 0 and 1 are possible. The model based upon the square wave or step function is structurally more attractive; the fit is only worse since the fourth-order satellites were not taken into account.

Cationic ordering

Fig. 3 (lowest part) presents a projection upon the $y = 0.25$ plane of a part of one Te sandwich of the modulated structure along the running direction of the modulation wave. One sheet of the Te sandwich is above the plane of projection, whereas the other is underneath. The remarkable square coordination of Si in the middle of the face shared by two trigonal Te prisms can be seen as well as the occurrence of both Ta—Ta bonded pairs and 'lone' Ta atoms in the middle of a trigonal prism. Three different subunits can be distinguished: the first with a Ta—Ta pair in the lower part and Si in the upper part, the second with a pair in the upper part and the Si in the lower part and the third with a lone Ta in both the lower and upper parts. The sequence of the subunits in one row (*e.g.* the lower row) of trigonal prisms along the running direction of the modulation wave is

$$...Ta(1)]—[Si,Ta(1)—Ta(2),Ta(1)]—$$

$$[Si,Ta(1)—Ta(2),Ta(1)]—$$

$$[Si,Ta(1)—Ta(2),Ta(1)]—[Si...$$
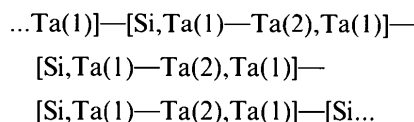
if the wavevector is exactly $q = 1/3c^*$. From this sequence it can be derived that the number of Si atoms is exactly equal to the number of Ta(2) atoms and that the mean occupancy of both sites is 1/3. The building block consisting of the three different subunits is drawn with its schematic representation in the upper part of Fig. 3. Incommensurateness can be introduced in this sequence by inserting quasi-periodic and uniformly distributed (100) faults. In this particular case the faults are to be defined as orthorhombic units with nominal composition Ta_2SiTe_4 consisting of only two subunits; the subunit with the lone Ta atoms is missing (Fig. 3).
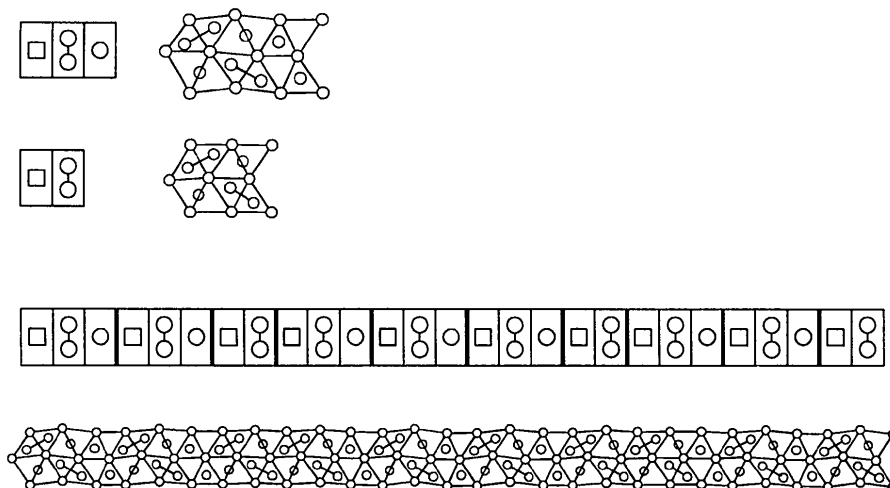
The problem of incommensurateness due to the quasi-periodic insertion of structural faults has already been discussed by Fujiwara (1957). Such structures are now called periodic anti-phase or interface-modulated structures; the latter seems more appropriate to our structure. The theory as developed by Fujiwara and later applied and extended by Van Dyck, Conde & Amelinckx (1979) can be used in our case to relate the value of the q vector to the composition of the modulated structure. Starting from the commensurate superstructure of Ta_3SiTe_6 with $q = 1/3c^*$ and the superstructure of Ta_2SiTe_4 with $q = 1/2c^*$, the q vector for structures intermediate of these is given by $q = \gamma c^*$,

$$\gamma = \frac{1}{3} + \delta = \frac{1}{3} + \frac{1}{jM} = \frac{1}{3} + \frac{1}{3M} = \frac{M+1}{3M}, \quad (8)$$

where M is the average spacing of the faults in multiples of the basic unit cell of the commensurate superstructures and j is the number of faults that must be crossed to regain the same structural position. The latter is three in our case since the insertion of one Ta_2SiTe_4 block corresponds with the removal of one subunit of the Ta_3SiTe_6 block. The overall composition of the structure based upon an average fault spacing of M is equal to the sum of $(M - 2)/3$ units of Ta_3SiTe_6 plus 1 unit of Ta_2SiTe_4 yielding $TaSi_{(M+1)/3M}Te_2$ or, more elaborated, $Ta(1)_{(2M-1)/3M}Ta(2)_{(M+1)/3M}Si_{(M+1)/3M}Te_2$. Thus, the occupancy is just equal to the value of γ. This is indeed to a close approximation of what is observed for refinement II when the occupancies are left free, even for a light element such as Si. The average fault spacing is calculated to be 12.41.

An alternative, but almost equivalent way of looking at the structure is by means of discommensurations or solitons, that is regions in the crystal

Fig. 3. Ordering pattern of Ta(1), Ta(2) and Si in one Te sandwich along the running direction of the modulation wave. Indicated are the units consisting of three subunits ('TaSi$_{1/3}$Te$_2$') and two subunits ('TaSi$_{1/2}$Te$_2$'), together with their schematical representations. Below, two examples are given of part of the sequence in its schematical and structural form.

that separate domains in which the structure is commensurate and where the global phase of the modulation wave is constant (Janssen & Janner, 1987). At the domain walls the global phase jumps to a new value. In our case, the domains consist of the modulated structure with $q = 1/3c^*$; at the domain wall the phase jumps with $\Delta(t) = 1/3$.

Discommensurations may move upon changing the temperature, and accordingly the wave vector may change in direction and/or magnitude. Finally, the structure can lock-in to a commensurate phase. This was elegantly shown by high resolution electron microscopy (HREM) experiments for the case of NbTe$_4$ (Mahy, Van Landuyt, Amelinckx, Bronsema & Van Smaalen, 1986), a compound with exclusively displacive modulation waves. In the case of TaSi$_{0.360}$Te$_2$ a temperature-dependent q vector caused by temperature-induced movements of discommensurations is more difficult to imagine. This would involve the movement of atoms over a length scale comparable to one basic unit cell, which is not felt likely. The incommensurateness of the structure of TaSi$_{0.360}$Te$_2$ stems from a compositional variation. Thus, the value of γ can only be commensurate if the number of lattice sites that is available for ordering in an integral number of basic unit cells is compatible with the number of cations to be accommodated.

Variation of interatomic distances

Figs. 4–7 present plots of interatomic distances *versus* the phase $t = \bar{x}_4 - q.r_0^\nu$ of the modulation wave. Te—Te distances (Figs. 4–5) can be divided into three subclasses, according to the presentation in electronic band structure calculations for the M—A—Te family of compounds (Canadell *et al.*, 1993; Evain *et al.*, 1994). Figs. 4(a)–4(c) give close Te—Te distances parallel to the sandwiches within one sheet, Figs. 5(a) and 5(b) present the distances through the van der Waals gap between the Te sheets of two adjacent sandwiches, and Figs. 5(c) and 5(d) give those through the sandwich from one sheet to the other. A striking modulation with an amplitude of about 0.4 Å is found for the Te—Te vector that crosses (in projection, see Figs. 1 and 3) the Si atom. The distance amounts to 4.10 Å for phases of the *modulation at which the Si occupancy is a maximum* to 3.25 Å at phases at which Ta(1)—Ta(2) pairs are found. It is noted that a Te—Te modulation of comparable size is found in the incommensurately modulated structure of calaverite, AuTe$_2$ (Schutte & de Boer, 1988), but that the minimal Te—Te distance is even smaller (2.82 Å). The two other in-plane Te—Te distances vary less and it is more difficult to assign a certain maximum or minimum to a structural feature like a particular point in the cationic distribution. At this stage some remarks about the

meaning of the maxima and minima in Figs. 4–7 and the distances in between should be made. It is noted that one expects a block-wave character for the modulation of the Te—Te distances as we have found for the occupational modulation waves, since the displacements of Te respond to the ordered arrangement of the cations. So, in fact, one needs for the refinement of all displacement-modulation waves the use of step functions resembling that of (5), but involving more than two steps and variable heights, or in other words, a piecewise constant function. In the framework of the discommensuration model one expects such piecewise constant modulation functions (Janssen & Janner, 1987). A refinement of this model was not tried in the present work. Thus, it is likely that the maximal and minimal values of the distances presented in Figs. 4–7 are slightly too high and low, respectively, since the modulations represent only the principal harmonics of the modulation wave. Nevertheless, it is instructive to monitor at least the most important deviations from the average structure. It is seen in Figs. 4–7 that the most prominent extrema occur at the phase $t \approx 0.30$. The intergap Te—Te distance is both minimal (Fig. 5b) and maximal (Fig. 5a), whereas the intrasandwich distance is minimal (Figs. 5c and 5d). These extrema are easily understood by steric arguments. At this phase of the modulation wave Si is found in its peculiar square coordination in the middle of the face shared by two trigonal prisms. This must impose strong distortions on the Te framework near this biprism.

Distances agree well with comparable distances found in the parent commensurate phase TaSi$_{1.3}$Te$_2$
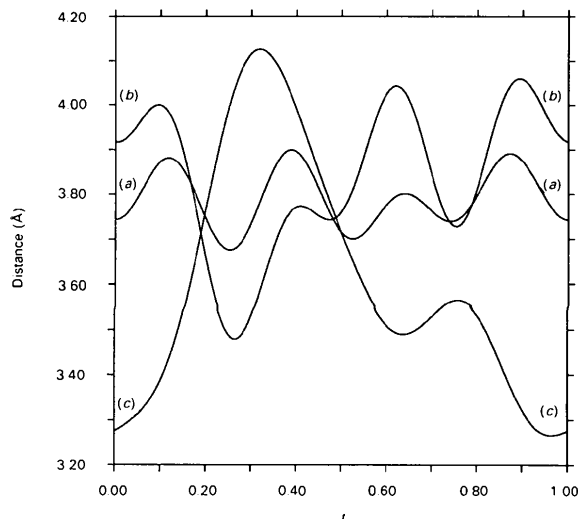
Fig. 4. Te—Te distances as a function of phase t of the modulation wave, from Te(x, y, z) to (a) Te($\frac{1}{2} + x, y, \frac{3}{2} + z$), ($b$) Te($\frac{1}{2} + x, y, 1 + z$) and ($c$) Te($\frac{1}{2} + x, y, \frac{1}{2} - z$).

(Evain *et al.*, 1994). The Ta(1)—Ta(2) distance (Fig. 7a) does not seem to be very reliable where the slope of the modulation curve becomes very steep. This is another indication that one should actually use piecewise constant displacive modulation functions in the refinement of this structure. Ta(1)—Te distances (Fig. 6) show a strong or weak modulation, depending whether Ta(1) is 'lone' or paired to Ta(2). Minima and maxima are found to be slightly lower
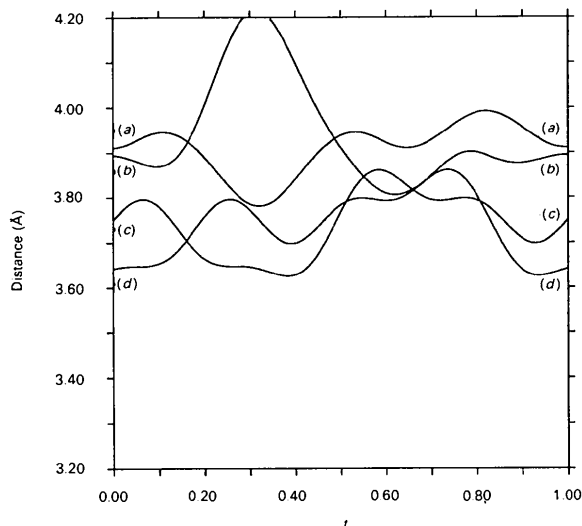
Fig. 5. Te—Te distances as a function of phase t of the modulation wave, from Te(x, y, z) to (a) Te($- x, - y, 1 - z$), (b) Te($\frac{1}{2} - x, - y, -\frac{1}{2} + z$) and (c) Te($x, \frac{1}{2} - y, z$); from Te($\frac{1}{2} + x, y, \frac{1}{2} - z$) to (d) Te($\frac{1}{2} + x, \frac{1}{2} - y, \frac{1}{2} - z$). (a) and (b) are interlayer distances, and (c) and (d) intralayer distances, *i.e.* through the sandwich.
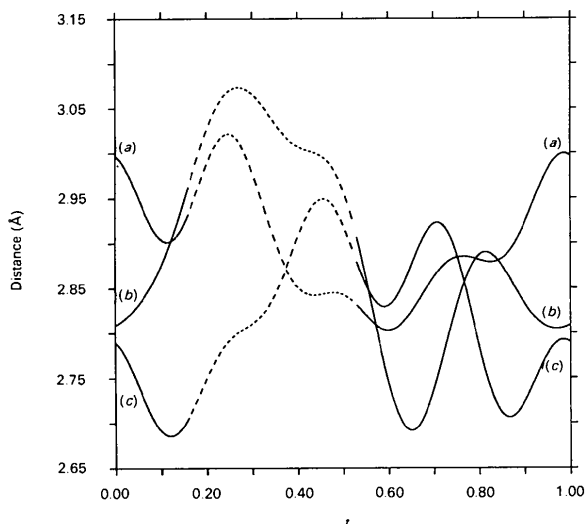
Fig. 6. Ta(1)—Te distances as a function of phase t of the modulation wave, from Ta(1)(x, y, z) to (a) Te(x, y, z), (b) Te($\frac{1}{2} + x, y, \frac{1}{2} - z$) and (c) Te($x, y, z - 1$). The curves are dashed where the occupancy of Ta(1) is equal to 0.00.

and higher, respectively, than for comparable distances in TaSi$_{1/3}$Te$_2$.

As was shown earlier (Monconduit *et al.*, 1992), the oxidation states of Ta and Si can be assigned the values $+3$ and $+2$, respectively. Accordingly, we are left with a fractional oxidation state of -1.860 for Te, which implies Te—Te bonding to be present in the structure. These Te—Te bonds need not correspond with the shortest inequivalent bonds found in Figs. 4 and 5. It was shown earlier (Canadell *et al.*, 1992; Canadell *et al.*, 1993) that Te p orbitals perpendicular to the sandwich are much more efficient than in-plane Te p orbitals in promoting electronic charge to the metal d-block band. Thus, the contribution of the shortest Te—Te contact present in the structure (in-plane: 3.24 Å) to the electronic charge transfer from the p- to d-block bands is estimated to be much smaller than the much larger Te—Te contact of 3.7 Å that is in between two successive sandwiches (Evain *et al.*, 1994). The origin of the occurrence of the very short in-plane Te—Te contact is therefore not yet known.

Concluding remarks

The incommensurate structure of TaSi$_{0.360}$Te$_2$ is found to be the ordered compromise between the orthorhombic modulated structures of TaSi$_{1/3}$Te$_2$ and TaSi$_{1/2}$Te$_2$. Since the latter can be regarded as TaSi$_{1/3}$Te$_2$ minus one subunit of composition TaTe$_2$, the stereochemistry of TaSi$_{0.360}$Te$_2$ is not very different from that of TaSi$_{1/3}$Te$_2$. The deviations of the
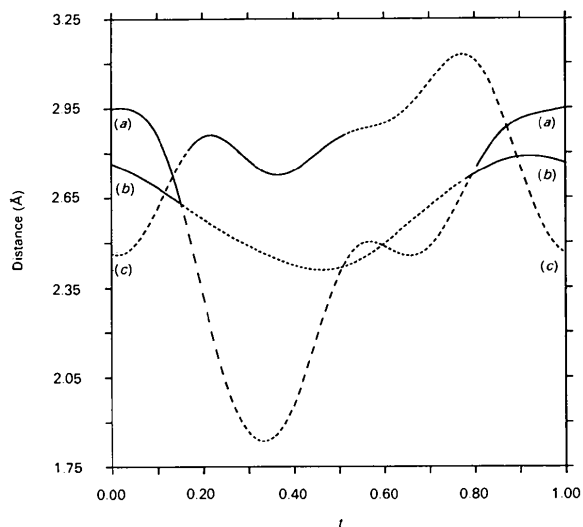
Fig. 7. Metal–metal distances as a function of phase t of the modulation wave, from Ta(1)(x, y, z) to (a) Ta(2)($\frac{1}{2} + x, y, \frac{1}{2} - z$), (b) Ta(1)($x, y, z$) to Si($-\frac{1}{2} + x, y, \frac{1}{2} - z$) and (c) Ta(2)($x, y, z$) to Si($x, y, z$). The curves are dashed where the occupancy of at least one of the metals is 0.00.

satellite positions from the equivalent positions in the diffraction patterns of the two parent phases is directly related to the stoichiometry of the compound. Both occupational and displacement modulation waves exhibit a strong block-wave character. Refinements were also performed with block-wave parameters for the occupational waves instead of the usual principal harmonics and found to be consistent with the latter.

The fundamental inability of an accurate recording of all harmonics needed for the correct characterization of the various block waves is one of the reasons that the refinement of the model against the observed intensity data does not lower the overall R factor below 0.09. It can be shown that for block-wave types, or more general piecewise constant functions, the intensities of satellites do not vanish rapidly with increasing order n [Janssen & Janner, 1987, equation (6)]. This causes the intensity due to the modulation to be spread over a large number of relatively weak reflections. These are normally measured with less accuracy than the strong main reflections, making the overall fit less accurate. Other reasons for the relatively large R factor, inherent to the two-dimensional character of the system, are the well-known presence of stacking faults in the structure and the very asymmetric shape of the crystal in conjunction with a high linear absorption coefficient of 510 cm^{-1}.

The research of AvdL has been made possible by a grant from Conseil Régional des Pays de la Loire and of VP by grant 202/93/1154 from the Grant Agency of the Czech Republic.

References

Böttcher, P. (1988). Angew. Chem. 100, 781–794.

Canadell, E., Jobic, S., Brec, R., Rouxel, J. & Whangbo, M.-H. (1992). J. Solid State Chem. 99, 189–199.
Canadell, E., Monconduit, L., Evain, M., Brec, R., Rouxel, J. & Whangbo, M. (1993). Inorg. Chem. 32, 10–12.
Evain, M. (1992). U-FIT. A Program for the Least-Square Refinement of Cell Parameters and Modulation Vectors. IMN, Laboratoire de Chimie des Solides, 44072 Nantes CEDEX 03, France.
Evain, M., Monconduit, L., Van der Lee, A., Brec, R., Rouxel, J. & Canadell, E. (1994). New J. Chem. In the press.
Fujiwara, K. (1957). J. Phys. Soc. J. 12, 7–13.
Hall, S. R., Flack, H. D. & Stewart, J. M. (1992). Editors. XTAL3.2 Reference Manual. Univs. of Western Australia, Australia, Geneva and Maryland, USA.
Janssen, T. & Janner, A. (1987). Adv. Physics 36, 519–624.
Jobic, S., Brec, R. & Rouxel, J. (1992). J. Alloys Compd. 178, 253–283.
Li, J., Badding, E. & DiSalvo, F. J. (1992). J. Alloys Compd. 184, 257–263.
Li, J. & Carroll, P. J. (1992). Mater. Res. Bull. 27, 1073–1081.
Mahy, J., Van Landuyt, J., Amelinckx, S., Bronsema, K. D. & van Smaalen, S. (1986). J. Phys. C, 19, 5049–5069.
Mar, A., Jobic, S. & Ibers, J. A. (1992). J. Am. Chem. Soc. 114, 8963–8971.
Monconduit, L., Evain, M., Boucher, F., Brec, R. & Rouxel, J. (1992). Z. Anorg. Allg. Chem. 616, 1–6.
Monconduit, L., Evain, M., Brec, R., Rouxel, J. & Canadell, E. (1993). C. R. Acad. Sci. 314, 25–34.
Petříček, V. (1993). JANA93. Programs for Modulated and Composite Crystals. Institute of Physics, Praha, Czech Republic.
Rouxel, J. (1993). Comments Inorg. Chem. 14, 207–228.
Schutte, W. J. & de Boer, J. L. (1988). Acta Cryst. B44, 486–494.
Smaalen, S. van (1993). Unpublished. Lab. of Chemical Physics, Univ. of Groningen, The Netherlands.
Van Aalst, W., Den Hollander, J., Peterse, W. J. A. M. & de Wolff, P. M. (1976). Acta Cryst. B32, 47–58.
Van der Lee, A., Evain, M., Monconduit, L., Brec, R. & van Smaalen, S. (1994). J. Phys. Condens. Matter. In the press.
Van der Lee, A., van Smaalen, S., Wiegers, G. A. & de Boer, J. L. (1991). Phys. Rev. B, 43, 9420–9430.
Van der Lee, A., Mansuetto, M., Evain, M., Monconduit, L., Brec, R. & Rouxel, J. (1994). J. Solid State Chem. In the press.
Van Dyck, D., Conde, C. & Amelinckx, S. (1979). Phys. Status Solidi A, 56, 327–334.
Yamamoto, A. (1981). Acta Cryst. A37, 838–842.

Effect of Lanthanide Contraction on the Structures of the Decatungstolanthanoate Anions in K3Na4H2[LnW10O36].nH2O (Ln = Pr, Nd, Sm, Gd, Tb, Dy) Crystals

By Tomoji Ozeki and Toshihiro Yamase

Research Laboratory of Resources Utilization, Tokyo Institute of Technology, 4259 Nagatsuta, Midori-ku, Yokohama 227, Japan

Abstract

Structures of tripotassium tetrasodium dihydrogen decatungstolanthanoate crystals, K3Na4H2[LnW10O36].- nH_2O (Ln = Pr, Nd, Dy; n = 21–22), have been determined and compared with the structures of their isomorphous crystals with Ln = Sm, Gd and Tb. K3Na4H2[PrW10O36].22H2O crystallizes in monoclinic,